Original Research

Double-Reference Cross-Correlation Algorithm for Separation of the Arteries and Veins From 3D MRA Time Series

Francesco Santini, MSc,[1]* Sunil Patil, MSc,[1] Stephan Meckel, MD,[2] Klaus Scheffler, PhD,[1] and Stephan G. Wetzel, MD[2]

Purpose: To present a novel postprocessing technique for artery/vein separation and background suppression from contrast-enhanced time-resolved magnetic resonance angiography datasets in order to improve the diagnosis of vessel pathologies and arteriovenous fistulas.

Materials and Methods: Ten normal, two pathologic datasets of the brain, and one hand angiography dataset were postprocessed. Cross-correlation maps between the signal time course of every voxel in the dataset and selected arterial and venous references regions of interest (ROIs) were obtained; these maps were subsequently nonlinearly transformed to obtain two indices representing the likelihood of a voxel belonging to a vessel category. Red-green-blue (RGB) color encoding was utilized to depict synthetic arteriogram and venogram images in a single diagnostically meaningful image.

Results: The technique enabled correct visual separation of vessels on various datasets, as evaluated by two expert neuroradiologists, and also highlighted characteristics of flow in arteriovenous fistulas. A quantitative comparison with existing techniques showed better separation performance on 3 out of 10 normal datasets and higher stability to acquisition characteristics and contrast agent bolus dispersion.

Conclusion: This method can be helpful in the diagnosis of vascular diseases in subjects where bolus dispersion makes it difficult to discriminate between arteries and veins with standard methods (subtraction or correlation analysis).

Key Words: contrast-enhanced MRA; artery/vein separation; correlation; fistula detection
J. Magn. Reson. Imaging 2008;28:646–654.

TIME-RESOLVED CONTRAST-ENHANCED magnetic resonance angiography (CE-MRA) (1–3) with high temporal resolution has become a widely used technique to visualize the dynamic transit of a contrast bolus from the arterial to the arteriovenous phase. To improve the visualization of vascular structure compared to background, usually magnitude or complex subtraction is performed (4). This method, either implemented as a 2D or 3D sequence, has been extensively used, for example, for the work-up of neurovascular disorders (eg, arteriovenous fistula) (5–11). However, there are important limitations of the technique. First, due to the short arteriovenous transit time (eg, 8 sec for the cerebral vessels) and the small diameter of many important vessels, there is a trade-off between the spatial and temporal resolutions of CE-MRA even if accelerated MR acquisitions with parallel imaging techniques are used. Second, in contrast to intra-arterial digital subtraction angiography (DSA), due to the arterial overlay in the venous phase, a separation of the arterial and venous phase is not possible, but merely the separation of an arterial and an "arteriovenous" phase. A display of the venous phase without superimposition of arteries is yet of interest for the evaluation of numerous vascular disorders.

Different postprocessing strategies have been proposed to deal with this task (12–19). The most commonly applied is the simple subtraction of the arterial datasets from venous datasets. However, the signal-to-noise ratio (SNR) in the resultant image is reduced by a factor of $\sqrt{2}$ if noise properties of the two images are similar. A method termed cross-correlation (12) was shown to be superior compared to the subtraction method both in terms of artery/vein separation and SNR. With this technique, the signal intensity time course of a region of interest (ROI) placed within an artery (vein) is cross-correlated with the time courses of all acquired datasets. The cross-correlation as an

[1]Division of Radiological Physics, Institute of Radiology, Basel University Hospital, University of Basel, Basel, Switzerland.
[2]Neuroradiology, Institute of Radiology, Basel University Hospital, University of Basel, Basel, Switzerland.
Contract grant sponsor: Swiss National Science Foundation; Contract grant number: 320000-113492.
Presented at the 23rd Annual Scientific Meeting of ESMRMB, Warsaw, 2006.
*Address reprint requests to: F.S., Division of Radiological Physics, Institute of Radiology, Basel University Hospital, Petersgraben 4, 4031 Basel, Switzerland. E-mail: francesco.santini@unibas.ch
Received November 21, 2007; Accepted June 6, 2008.
DOI 10.1002/jmri.21499
Published online in Wiley InterScience (www.interscience.wiley.com).

index of similarity ideally yields an arteriogram (venogram) only. This technique also leads to an increase in SNR by a factor of about two with respect to the subtraction technique. The implicit assumption of this technique is that the temporal behavior of the arterial phase does not overlap with the temporal behavior of venous phase significantly. However, this assumption is not always fulfilled and an unwanted depiction of venous signal in the arteriogram and vice versa can be observed.

In this article an extension of the standard cross-correlation technique, here termed double-reference cross-correlation, is presented. An algebraic transformation is applied to the cross-correlation maps in order to compensate for the mutual correlation of the reference time courses. Subsequently, a red-green-blue (RGB) color map is applied in order to represent the whole angiogram in one synthetic image depicting arteries and veins in different colors.

In the first part of the article the theoretical bases of cross-correlation and double-reference cross-correlation are explored. In the second part the method is qualitatively and quantitatively compared with the already established cross-correlation technique, in the analysis of time-resolved MRA of cerebral datasets. In the pool of datasets, both subjects without pathologies as well as patients suffering from a dural arteriovenous malformation were included. As a further example the postprocessing algorithm was also applied to a time-resolved MRA of the hand.

MATERIALS AND METHODS

Theory

Standard Cross-Correlation Algorithm

The cross-correlation between a discrete test function T and discrete reference function R can be defined as:

$$c(T,R) = \frac{\sum_{i=0}^{N-1} (R(t_i) - \bar{R})(T(t_i) - \bar{T})}{\sqrt{\sum_{i=0}^{N-1} (R(t_i) - \bar{R})^2} \sqrt{\sum_{i=0}^{N-1} (T(t_i) - \bar{T})^2}}, \quad [1]$$

where N is the number of measured 3D volume datasets and $\bar{R}$, $\bar{T}$ are means of the corresponding series. The coefficient $c(T, R)$ is maximal if $T = R$.

The mean-detrended and normalized value of a function T can be defined as:

$$\hat{T}(t_i) = \frac{T(t_i) - \bar{T}}{\sqrt{\sum_{i=0}^{N-1} (T(t_i) - \bar{T})^2}}. \quad [2]$$

Defining $\hat{R}$ in a similar way we obtain:

$$c(T,R) = \hat{T} \cdot \hat{R}, \quad [3]$$

which is the scalar product between the two vectors $\hat{T}$ and $\hat{R}$. The correlation coefficient c is always in the interval $[-1, 1]$, being the scalar product between two vectors of unit norm. In general, the correlation coefficients are the cosine of the angle between the reference and test vector in N-dimensional space of the discrete time courses. Because of the normalization procedure of the test vector, the temporal behavior of the signal (for, eg, vascular structure) as well as background falls into the same dynamic range. This is undesirable, as it discards the actual signal strength information (gray level value in the original image) of the test vector. Hence, in order not to lose SNR in the resultant correlation map the scalar product between the normalized reference vector and nonnormalized test vector is computed, ie, $\tilde{T}(t) = T(t_i) - \bar{T}$.

Thus, the formula for correlation coefficients becomes:

$$c(T,R) = \tilde{T} \cdot \hat{R}. \quad [4]$$

Double-Reference Cross-Correlation

With the standard cross-correlation technique, the cross-correlated coefficient can be interpreted as the length of the projection of the time course of the test vector on the axis of the reference vector. The correlation maps obtained with respect to arterial reference and venous reference are treated as independent of each other. However, because of significant overlapping of arterial and venous phase, there is sometimes a mutual dependency between the two correlation maps. In this case the arterial and venous reference time courses become similar to each other, and therefore the resulting correlation maps will show little difference. In the double-reference cross-correlation technique this dependency is decoupled by formulating the relation between the considered reference vectors. The aim of this approach is to classify a voxel as "arterial" or "venous" as the result of a comparison between the measures of similarity of the voxel time course with the arterial and venous references, represented by the standard cross-correlation maps. The classifier also uses a "soft margin" approach instead of a hard thresholding in order to take into account for voxels with mixed arterial and venous time courses.

The classification is obtained through a nonlinear transformation of the correlation maps and through an application of an RGB color map to the transformed values.

Consider a 2D subspace formed by two reference vectors, which is called a "vessel plane." The two reference vectors form on this plane an angle $\theta = \arccos(R_{artery} \cdot R_{vein})$ that is given by the arc cosine of the correlation coefficient between the references, which we termed the "skew angle" (see Fig. 1a).

The length of the projection vector of time course of the test vector onto this plane gives the signal strength information. The direction angle comparison with the skew angle indicates whether it is a part of an artery or a vein. The coordinates of projection vector in this plane are the cross-correlation coefficients $c(T, R_{artery})$ and $c(T, R_{vein})$ of the time course of the test vector obtained with

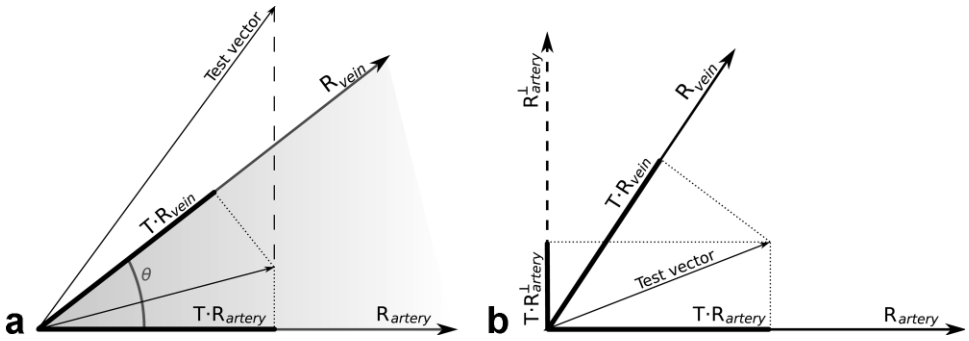

Figure 1. a: Vector representation of correlation coefficients in the standard cross-correlation technique. The correlation coefficients are projections of the test vector on the reference axes. The test vector components that are not coplanar with the references are discarded in the projection process. The "skew angle" θ is also shown. **b:** Orthogonal transformation of reference system. From the projection of test vector on the arterial and venous reference another coefficient is calculated, corresponding to the projection of vector on the axis normal to the arterial reference.

respect to arterial reference and venous reference, respectively.

Thus, the calculation of length and direction of any vector in the vessel plane can be performed provided its cross-correlation coefficients are known. In order to simplify this algebraic manipulation, the vessel plane is converted into an orthonormal (rectangular) coordinate system. Although any arbitrary orthonormal system can be chosen, for simplicity an orthonormal system formed by (R_{artery}, $R^{\perp}_{artery}$) is chosen (Fig. 1b). The coordinates of any vector in the new orthonormal system can be calculated from the correlation coefficients using the coordinate transformation formula given by (see Appendix):

$$\begin{bmatrix} T_{R_{artery}} \\ T_{R^{\perp}_{artery}} \end{bmatrix} = \begin{bmatrix} 1 & 0 \\ -\cot(\theta) & \csc(\theta) \end{bmatrix} \begin{bmatrix} c(T,R_{artery}) \\ c(T,R_{vein}) \end{bmatrix}, \quad [5]$$

where $T_{R_{artery}}$ and $T_{R^{\perp}_{artery}}$ are coordinates of the test vector in the new orthonormal reference system, and θ is the skew angle. The calculation of the length and direction of any vector in this rectangular coordinate system may be done by converting it into a polar coordinate system. The rectangular to polar coordinate transformation is given by:

$$r = \sqrt{(T_{R_{artery}})^2 + (T_{R^{\perp}_{artery}})^2}, \quad [6]$$

$$\alpha = \text{sign}(T_{R^{\perp}_{artery}})\arccos\left(\frac{T_{R_{artery}}}{r}\right), \quad [7]$$

where $0 \leq r < \infty$ and $-\pi < \alpha \leq \pi$.

In order to form an image from length r and direction angle a, color map encoding may be used.

RGB Encoding

The color maps have more degrees of freedom as compared to gray-level maps. For example, an RGB map synthetically represents three gray-level maps in one image. In the present case, two scalar values, the vector length r and the direction angle α, corresponding to each voxel are encoded using RGB color map. The RGB color map encoding leads to simultaneous visualization of both arteriogram (red) and venogram (blue), otherwise impossible with gray-level encoding.

The parameter α is an angle between a vector and the arterial reference in an orthogonal system formed by arterial and venous reference. Hence, it indicates the proximity of that vector with either the arterial reference or the venous reference. The comparison of the bisector of skew angle between arterial reference and venous reference and a categorizes the vector as part of an arteriogram (red) or a venogram (blue). If α is much higher than the arterial or venous reference direction angle, the voxel is identified as noise and mapped as background signal (black). Parameter r represents the length of the projection of the test vector onto the vessel plane. Therefore, it is directly mapped as brightness of the voxel.

Figure 2 shows the color assigned by our implementation of the algorithm to each vector lying on the vessel plane using the RGB color map. The region in proximity to the bisector of skew angle appears purple in color due to mixed mapping of red and blue colors.

Image Acquisition and Implementation Details

To evaluate the double-reference cross-correlation technique, ten randomly chosen time-resolved 3D cerebral CE-MRA datasets from patients in whom neurovascular disease was ruled out by MR and MRA workup were included in this analysis. In addition, two datasets from patients with a cerebral dural arteriovenous fistula as proven by DSA and a dataset from a time-resolved MR angiography of the hand were included. This retrospective analysis of the patient data was approved by the local ethics commission.

MR Image Acquisition Specification and Data Postprocessing

Cerebral time-resolved 3D-MRA datasets used for this study were acquired using 3D FLASH sequence implemented on a 1.5T MRI system (Magnetom Avanto, Siemens Medical Solutions, Erlangen, Germany) with the same scanning parameters as de-

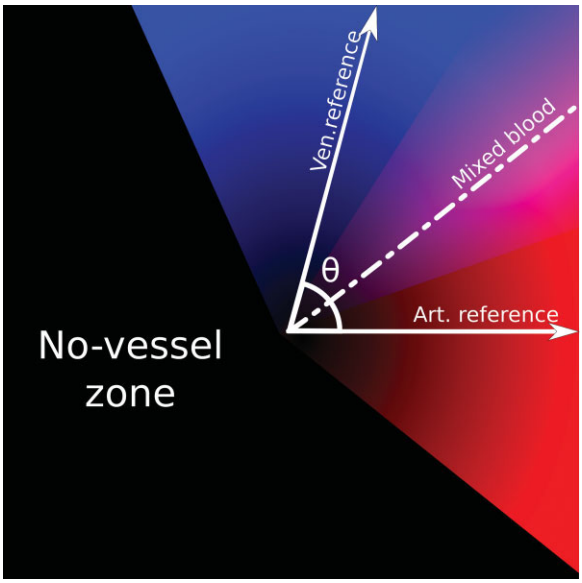

Figure 2. The RGB color encoding of the vessel plane. The skew angle θ is indicated as the angle between the reference directions. Four zones are identified in the plane, a pure arterial blood zone (red), where phase ranges from –θ/2 to θ/4; a mixed blood zone (purple), with range θ/4, 3/4 θ; a pure venous blood zone (blue), with range 3/4 θ, 3/2 θ; and a "no-vessel" zone (black), ranging outside the aforementioned ones.

scribed by Meckel et al (5,11). An in-plane resolution of 2.0 × 2.0 mm with a slice thickness of 2.2 mm and a temporal resolution of 1.5 seconds per 3D dataset were obtained. A single bolus of contrast agent (0.5 molar gadolinium-DOTA) was administered using a power injector (20 mL, 3 mL/s) followed by a saline flush. In total, a series of 25 3D datasets were acquired in 37.5 seconds, where the acquisition of the first dataset was started simultaneously with the injection of the contrast agent bolus. The hand dataset was acquired with the scanning parameters that were described in a study by Bilecen et al (20) with a spatial resolution of 0.62 × 1.14 × 1.00 mm^3 and a time resolution of 20 seconds per dataset.

The double-reference cross-correlation algorithm was implemented as ANSI C plug-ins for MatLab (MathWorks, Natick, MA). All programs were implemented on a 64-bit personal computer with 2 GB of RAM running GNU/Linux (kernel v. 2.6.12) operating system. The effective computation time with this configuration was less than a minute for each dataset. The arterial reference was chosen as an ROI placed into the internal carotid artery and the venous reference was chosen in the superior sagittal sinus.

To evaluate the effect of time resolution on the separation performance, one dataset was downsampled from the original time resolution (1.5 sec) to lower sampling periods (3.0, 4.5, 6.0, and 7.5 sec) to mimic multiple acquisitions at different time resolutions. The cross-correlation and the double-reference cross-correlation algorithms were then independently applied on all obtained datasets.

In order to directly compare the results of the double-reference cross-correlation algorithm with the cross-correlation technique, gray-level maps were also calculated from the RGB images. This was achieved by alternatively selecting the red channel and the blue channel information for direct comparison with the standard cross-correlation algorithm and quantitative analysis.

Data Analysis and Quality Assessment

The results of the double-reference cross-correlation algorithm were presented to two experienced radiologists for qualitative evaluation as red-green-blue maximum intensity projection (MIP) images. They were asked to decide whether the artery/vein separation was correct, and to identify and describe possible pathologies.

Quantitative assessment of the separation efficiency was evaluated by calculating the contrast between arteries and veins in the arterial and venous gray-level maps. For this purpose the sagittal maximum intensity projections (obtained with the double-reference cross-correlation and with the cross-correlation algorithms) were calculated, and ROIs were selected in the arteries of the circle of Willis and in the superior sagittal sinus. Special attention was taken so to select areas where arteries and veins do not overlap in the projection. The mean intensities of the ROIs were calculated in the calculated arterial map and in the calculated venous map. The contrasts were calculated as artery/vein intensity ratio between the values obtained from the arterial map, and as vein/artery intensity ratio between the values obtained from the venous map. With this method, four values were obtained for each dataset, ie, AVR_{DRCC}, AVR_{SCC}, VAR_{DRCC}, and VAR_{SCC}, respectively, representing the artery/vein contrast in the double-reference cross-correlation arterial map, the artery/vein contrast in the cross-correlation arterial map, the vein/artery contrast in the double-reference cross-correlation venous map, and the vein/artery contrast in the cross-correlation venous map. In case of perfect separation, these indices would all assume an infinite value. The results were compared by calculating the difference between the contrast obtained with cross-correlation and the contrast obtained with double-reference cross-correlation, divided by the contrast of the cross-correlation algorithm.

RESULTS

Visual Assessment of the Vessels

The radiologists reported a correct visual separation of arteries and veins using the double-reference cross-correlation algorithm on all datasets. Examples are shown in Fig. 3, representing arteriograms and venograms of five datasets, and in Fig. 4, where the results obtained with the double-reference cross-correlation algorithm on the dataset of a normal subject are compared to the results deriving from the cross-correlation technique.

The improvement on the separation of arteries and veins was visually pronounced if the skew angle was low, indicating a high bolus dispersion, as shown in Fig. 5.

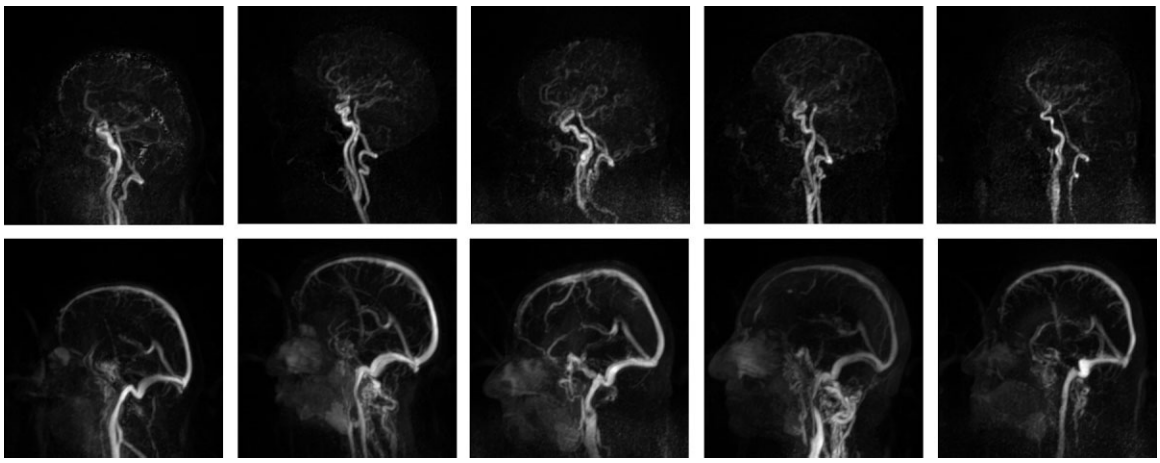

Figure 3. Sagittal grayscale MIPs of the arteriogram (top row) and venogram (bottom row) obtained by keeping alternatively the red and blue channel information of 3D RGB datasets of five normal subjects computed with the double-reference cross-correlation algorithm (skew angle values, from left to right: 44.0°, 86.4°, 93.6°, 115.8°, 129,6°).

In both datasets from patients suffering from dural cerebral arteriovenous fistulas, the radiologists were able to identify, in accordance to the findings from DSA, four "functional" types of vessels, as shown in Fig. 6. The arteries were depicted in red; the veins with normal (late) venous outflow in blue; the "arterialized" veins, ie, the veins with early filling with arterial blood due to the fistula, and no normal venous outflow in red; veins that showed early filling with arterial blood but also late venous outflow in purple.

The method was successful in the separation of arteries and veins also when applied to a time-resolved contrast-enhanced hand angiography dataset as shown in Fig. 7.

Quantitative Assessment

The performance of the double-reference cross-correlation algorithm was compared in the nonpathologic brain datasets with the standard cross-correlation algorithm by comparing the arteriogram artery/vein intensity ratio and the venogram vein/artery intensity ratio.

Out of 10 analyzed datasets, three showed a skew angle smaller than 90°, which is the theoretical threshold for the performance decay of the cross-correlation algorithm, as described in the Theory section.

In accordance to the qualitative results (Fig. 5), the performance for the double-reference cross-correlation algorithm is considerably higher than for the standard cross-correlation algorithm at low skew angles (<90°), while both algorithms have similar performance (difference <1%) at higher skew angles (Table 1).

As expected, the reduction in temporal resolution (increase of sampling period) of acquisition of the 3D MRA datasets also reduced the skew angle. As shown in Table 2, the double-reference cross-correlation algorithm outperformed the cross-correlation algorithm at lower temporal resolutions. In particular, at the lowest temporal resolution (7.5 sec) the double-reference cross-correlation had an improvement of up to 555% with respect to the standard cross-correlation algorithm.

DISCUSSION

In this work we presented a postprocessing algorithm for the separation of arteries and veins in time-resolved

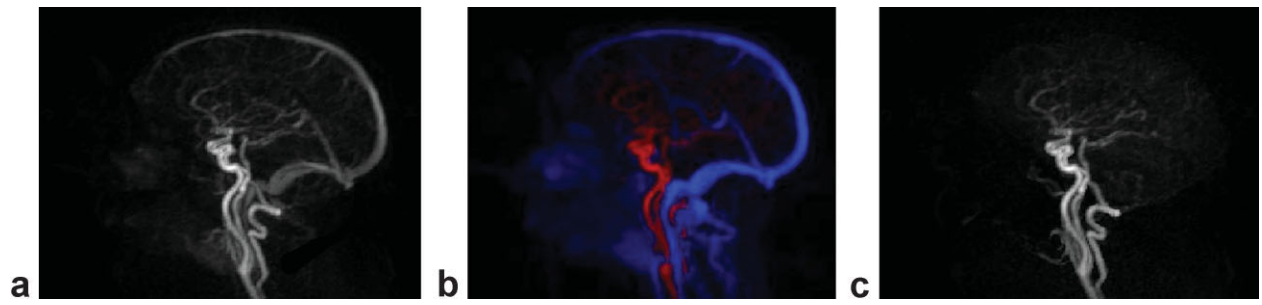

Figure 4. a: The MIP of arteriogram obtained using standard cross-correlation technique. In this case, the correlation value between arterial and venous reference was positive and a strong overlay of veins can be seen. **b:** Sagittal MIP representation of the entire angiogram of a normal subject, obtained using double-reference cross-correlation algorithm. Red channel is used to depict arteriogram and blue channel is used to depict venogram. **c:** Sagittal MIP of the arteriogram. The image was computed from the 3D RGB dataset generated by the algorithm by keeping the red channel information and displayed as a gray-scale MIP.

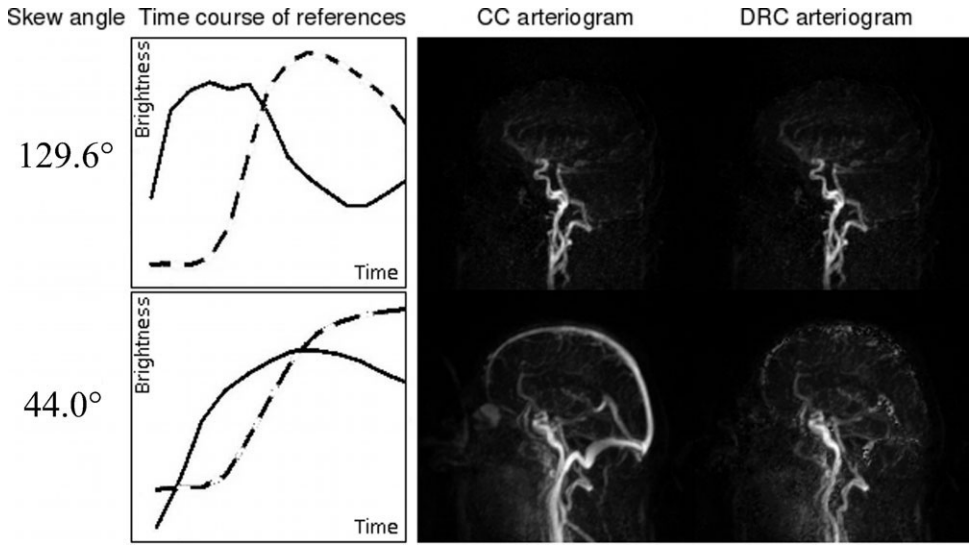

Figure 5. Different dispersion of contrast agent bolus in two subjects leads to different time courses of reference points (in solid line the arterial reference and in dashed line the venous reference). The upper panel shows that the standard cross-correlation (SCC) and double-reference cross-correlation (DRCC) algorithms have similar performance when the skew angle is higher (129.6°). The lower panel shows the performance of the two algorithms when the skew angle is lower (44.0°), which is an indicator of higher dispersion of the bolus. In this case the standard cross-correlation algorithm almost completely fails in separating the vessels, while double-reference cross-correlation succeeds, at the cost of lower SNR.

3D CE-MRA datasets, termed the double-reference cross-correlation technique, an extension of the already established cross-correlation technique (12). With this technique it was possible to improve the suppression of background structures and the separation of the arterial phase from the venous phase compared to the aforementioned technique. Utilizing an RGB color encoding technique a display of mixed blood effect in fistulas was made, and a consistent and reliable 3D or MIP display of both arteriogram and venogram was provided.

As expected from the theoretical derivations, the performance of the double-reference cross-correlation technique was equivalent to cross-correlation when the correlation between the two references is zero. When this correlation value is negative, the results are similar, provided that thresholding is applied to the output image of the cross-correlation algorithm. The advantage of the double-reference cross-correlation technique over the standard cross-correlation technique can be appreciated when the correlation value between the two references is positive. This happens when the contrast

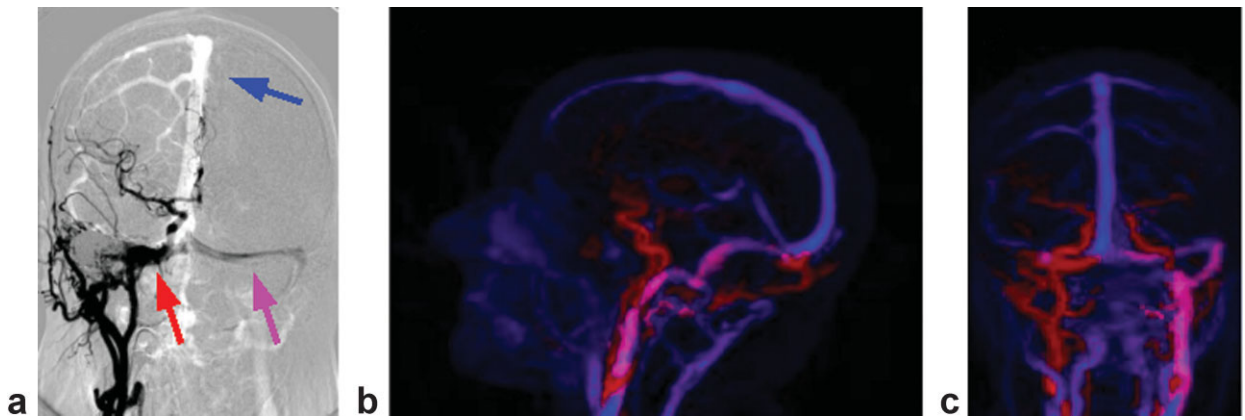

Figure 6. a: Mask subtracted conventional DSA image in anterior–posterior orientation of a patient with a dural fistula. The early appearing vessels appear black, the later ones white. Note that due to the fistula on the right side, the right transverse venous sinus appears early (red arrow) while the left transverse sinus shows a mixed black and white appearance (pink arrow). This indicates that shunted blood from the right side is mixed with the normal venous blood from the superior sagittal sinus (blue arrow). **b,c:** Sagittal and coronal MIP of a patient having a dural arteriovenous fistula involving the transverse sinus. The arteriovenous shunt is visible at the point where the occipital artery indicated in red enters into the right transverse sinus. The proximal part of the transverse sinus is depicted in red color indicating the arterialization of this vein. In addition, mixed blood flowing through the left jugular vein is highlighted in purple. The ipsilateral right jugular vein and sigmoid sinus is occluded after endovascular embolization therapy.

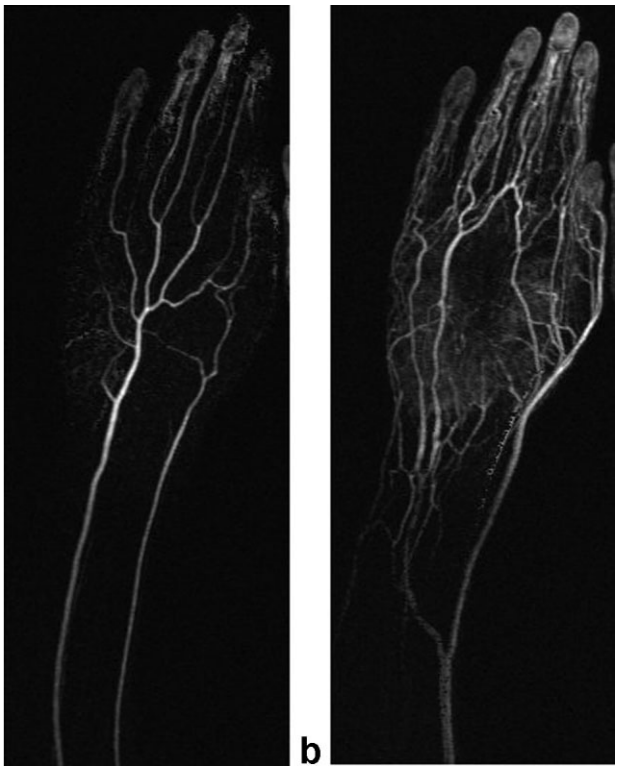

Figure 7. Example of arteriogram (**a**) and venogram (**b**) obtained from a time-resolved dataset of a hand in a normal subject.

agent bolus is dispersed due to subject's circulatory system characteristics or due to technical reasons, resulting in overlapping of the arterial and venous phase. An important feature of the double-reference cross-correlation algorithm is the robustness toward lower time resolution of the acquired datasets, which leads to higher correlation between the references.

A drawback of this algorithm is that it does not allow a real-time implementation, requiring all timepoints to be acquired before the processing. Moreover, a certain amount of user interaction is needed for reference selection, which increases the overall processing time.

Various other postprocessing algorithms for artery/vein separation utilizing time-resolved datasets are present in the literature (12,16,21). All these algorithms rely on measuring the similarity between the time course of the dataset voxels with some reference function. Kim and Zabih (21) described an approach termed the "model based segmentation," in which the temporal behavior of each time-series pixel was compared with a standard model such as a straight line or series of straight lines. As a major advantage, this method required no manual selection of a reference ROIs, as the reference waveform is a priori defined; however, this assumption, together with the assumption that the time series can be described as a series of straight lines, might lead to reduced performance in some cases as a trade-off for the lesser need for user interaction.

Another approach for artery/vein segmentation is based on different types of connectivity algorithms (13–15,17–19,22), which utilizes a high-resolution dataset to segment out the arteries and veins. It exploits the geometrical characteristics of the arterial and venous vessel trees, comparing the brightness of every voxel with its neighbors and thus deciding whether they belong to the same structure or not. Different decision-making algorithms lead to different implementations and different performances. Although similar in purpose, this class of techniques for artery/vein segmentation is very different from the class to which the double-reference algorithm belongs. In the former case, separation is obtained by pure image processing techniques and is directly related to the geometry of the acquired dataset, and not to the flow characteristics; it allows the acquisition of the MR dataset during the steady-state phase of the contrast agent, with longer scan times and higher resolution, because no time-resolved acquisition is needed. In the latter case, separation is obtained through the analysis of flow patterns as detected from a time-resolved scan, and therefore direct information about blood flow is obtained. For these reasons, direct comparison between these two classes of algorithms cannot be performed.

In conclusion, the results of the double-reference cross-correlation technique were promising for the application to CE-MRA, as shown in the example of neu-

Table 1
Comparison Between Double-reference Cross-correlation (DRCC) and Standard Cross-correlation (SCC) Algorithms for Datasets of 10 Different Subjects Having Different Values of Skew Angle

Skew angle [deg]	AVR_{SCC}	AVR_{DRCC}	Improvement	VAR_{SCC}	VAR_{DRCC}	Improvement
44.0°	1.03	9.24	799.73%	1.38	1.56	13.48%
60.5°	0.86	5.29	513.62%	3.61	4.14	14.87%
86.4°	7.04	14.57	106.90%	7.62	7.66	0.49%
93.6°	8.43	8.50	0.83%	7.42	7.42	0.01%
96.8°	11.86	11.86	0.00%	3.69	3.69	0.01%
100.2°	14.68	14.70	0.18%	4.08	4.08	0.05%
110.7°	6.54	6.53	−0.11%	4.03	4.03	−0.03%
115.8°	6.01	6.00	−0.06%	10.94	10.93	−0.03%
122.1°	18.40	18.38	−0.07%	5.00	5.00	0.01%
129.6°	14.19	14.18	−0.02%	2.80	2.80	0.00%

AVR_{SCC}, artery/vein contrast in the arteriogram calculated with cross-correlation; AVR_{DRCC}, artery/vein contrast in the arteriogram calculated with double reference cross-correlation; VAR_{SCC}, vein/artery contrast in the venogram calculated with cross-correlation; VAR_{DRCC}, vein/artery contrast in the venogram calculated with double reference cross-correlation.

Table 2
Separation Performance of the Double-reference Cross-correlation (DRCC) Algorithm Compared to the Standard Cross-correlation (SCC) Algorithm for the Same Dataset Sampled at Different Frame Rates and Thus Having Different Skew Angles

Time resolution [sec]	Skew angle [deg]	AVR_{SCC}	AVR_{DRCC}	Improvement	VAR_{SCC}	VAR_{DRCC}	Improvement
1.5	86.4°	7.04	14.57	106.90%	7.62	7.66	0.49%
3	79.6°	2.70	13.21	388.41%	6.81	7.02	3.12%
4.5	74.5°	1.95	11.83	506.28%	5.87	7.14	21.77%
6	68.1°	1.54	7.98	418.52%	4.52	7.74	71.21%
7.5	48.8°	0.93	6.10	555.81%	2.52	4.24	67.94%

rovascular applications. The ability of this algorithm to compensate for higher correlation between the selected reference time courses can be exploited to acquire datasets with lower time resolution and therefore higher spatial detail.

The application of the algorithm to other regions of the body, where bolus dispersion can be a more critical issue, is yet to be thoroughly studied. The analysis of a dataset of a time-resolved angiography of the hand, acquired with a significantly lower time resolution, showed encouraging results.

As an outlook, automation of reference selection will be hopefully implemented in order to completely remove the need of operator intervention and therefore increase the time efficiency of the algorithm.

APPENDIX

Derivation of the Coordinate Transformation Formula Given by Eq. [5]

Let T be the test vector considered. Let R_{artery} and R_{vein} be the reference vectors of unit norm. Let $R^{\perp}_{artery}$ be the vector of unit norm perpendicular to R_{artery}, on the Reference plane. Let $T_{R_{artery}}$, $T_{R_{vein}}$, $T_{R^{\perp}_{artery}}$ be the short forms for $T \cdot R_{artery}$, $T \cdot R_{vein}$, $T \cdot R^{\perp}_{artery}$, respectively.

Since R_{artery} and $R^{\perp}_{artery}$ form an orthonormal basis, T can be written as:

$$T = (T \cdot R_{artery})R_{artery} + (T \cdot R^{\perp}_{artery})R^{\perp}_{artery}, \qquad [12]$$

where $T \cdot R^{\perp}_{artery}$ is unknown. By taking the inner product with R_{vein} on both sides, we get:

$$T \cdot R_{vein} = (T \cdot R_{artery})(R_{artery} \cdot R_{vein}) + (T \cdot R^{\perp}_{artery}) \times (R^{\perp}_{artery} \cdot R_{vein}). \quad [13]$$

Considering that R_{vein} has unit norm in the $(R_{artery}, R^{\perp}_{artery})$ coordinate system, it is possible to calculate:

$$(R^{\perp}_{artery} \cdot R_{vein})^2 + (R_{artery} \cdot R_{vein})^2 = 1 \Rightarrow (R^{\perp}_{artery} \cdot R_{vein}) = \sqrt{1 - (R_{artery} \cdot R_{vein})} = \sqrt{1 - \cos^2\theta} = \sin\theta \quad [14]$$

The sign information is not taken into account because taking the opposite sign would mean considering the second reference axis as rotated by 180°, but the two references would still remain orthogonal, serving the purpose of this method. Therefore, the value of the second coordinate $T \cdot R^{\perp}_{artery}$ is:

$$T \cdot R^{\perp}_{artery} = \frac{T \cdot R_{vein} - (T \cdot R_{artery})}{(R_{artery} \cdot R_{vein}} = \frac{1}{\sin\theta} T \cdot R_{vein} - \frac{\cos\theta}{\sin\theta} T \cdot R_{artery} = -\cot(\theta)(T \cdot R_{artery}) + \csc(\theta)(T \cdot R_{vein}) \quad [15]$$

In matrix form this can be written as:

$$\begin{bmatrix} T \cdot R_{artery} \\ T \cdot R^{\perp}_{artery} \end{bmatrix} = \begin{bmatrix} 1 & 0 \\ -\cot(\theta) & \csc(\theta) \end{bmatrix} \begin{bmatrix} T \cdot R_{artery} \\ T \cdot R_{vein} \end{bmatrix}. \quad [16]$$

Using the short forms introduced above and using the definition of correlation (Eq. [4]), it can be written as:

$$\begin{bmatrix} T_{R_{artery}} \\ T^{\perp}_{Rartery} \end{bmatrix} = \begin{bmatrix} 1 & 0 \\ -\cot(\theta) & \csc(\theta) \end{bmatrix} \begin{bmatrix} c(T,R_{artery}) \\ c(T,R_{vein}) \end{bmatrix}. \quad [17]$$

REFERENCES

1. Korosec FR, Frayne R, Grist TM, Mistretta CA. Time-resolved contrast-enhanced 3D MR angiography. Magn Reson Med 1996;36: 345–351.
2. Prince MR. Contrast-enhanced MR angiography: theory and optimization. Magn Reson Imaging Clin N Am 1998;6:257–267.
3. Prince MR, Meaney JF. Expanding role of MR angiography in clinical practice. Eur Radiol 2006;16(Suppl 2):B3–8.
4. Naganawa S, Ito T, Iwayama E, et al. Magnitude subtraction vs. complex subtraction in dynamic contrast-enhanced 3D-MR angiography: basic experiments and clinical evaluation. J Magn Reson Imaging 1999;10:813–820.
5. Meckel S, Mekle R, Taschner C, et al. Time-resolved 3D contrast-enhanced MRA with GRAPPA on a 1.5-T system for imaging of craniocervical vascular disease: initial experience. Neuroradiology 2006;48:291–299.
6. Wetzel SG, Bilecen D, Lyrer P, et al. Cerebral dural arteriovenous fistulas: detection by dynamic MR projection angiography. AJR Am J Roentgenol 2000;174:1293–1295.
7. Aoki S, Yoshikawa T, Hori M, et al. MR digital subtraction angiography for the assessment of cranial arteriovenous malformations and fistulas. AJR Am J Roentgenol 2000;175:451–453.
8. Tsuchiya K, Aoki C, Fujikawa A, Hachiya J. Three-dimensional MR digital subtraction angiography using parallel imaging and keyhole data sampling in cerebrovascular diseases: initial experience. Eur Radiol 2004;14:1494–1497.
9. Ziyeh S, Strecker R, Berlis A, Weber J, Klisch J, Mader I. Dynamic 3D MR angiography of intra- and extracranial vascular malformations at 3T: a technical note. AJNR Am J Neuroradiol 2005;26:630–634.
10. Noguchi K, Melhem ER, Kanazawa T, Kubo M, Kuwayama N, Seto H. Intracranial dural arteriovenous fistulas: evaluation with combined 3D time-of-flight MR angiography and MR digital subtraction angiography. AJR Am J Roentgenol 2004;182:183–190.

11. Meckel S, Maier M, Ruiz DS, et al. MR angiography of dural arteriovenous fistulas: diagnosis and follow-up after treatment using a time-resolved 3D contrast-enhanced technique. AJNR Am J Neuroradiol 2007;28:877–884.
12. Bock M, Schoenberg SO, Floemer F, Schad LR. Separation of arteries and veins in 3D MR angiography using correlation analysis. Magn Reson Med 2000;43:481–487.
13. Lei T, Udupa JK, Odhner D, Nyul LG, Saha PK. 3DVIEWNIX-AVS: a software package for the separate visualization of arteries and veins in CE-MRA images. Comput Med Imaging Graph 2003;27: 351–362.
14. Lei T, Udupa JK, Saha PK, Odhner D. Artery-vein separation via MRA—an image processing approach. IEEE Trans Med Imaging 2001;20:689–703.
15. Lei T, Udupa JK, Saha PK, et al. 3D MRA visualization and artery-vein separation using blood-pool contrast agent MS-325. Acad Radiol 2002;9(Suppl 1):S127–133.
16. Martel AL, Fraser D, Delay GS, Morgan PS, Moody AR. Separating arterial and venous components from 3D dynamic contrast-enhanced MRI studies using factor analysis. Magn Reson Med 2003; 49:928–933.
17. Stefancik RM, Sonka M. Highly automated segmentation of arterial and venous trees from three-dimensional magnetic resonance angiography (MRA). Int J Cardiovasc Imaging 2001;17:37–47.
18. Tizon X, Smedby O. Segmentation with gray-scale connectedness can separate arteries and veins in MRA. J Magn Reson Imaging 2002;15:438–445.
19. van Bemmel CM, Spreeuwers LJ, Viergever MA, Niessen WJ. Level-set-based artery-vein separation in blood pool agent CE-MR angiograms. IEEE Trans Med Imaging 2003;22:1224–1234.
20. Bilecen D, Aschwanden M, Heidecker HG, Bongartz G. Optimized assessment of hand vascularization on contrast-enhanced MR angiography with a subsystolic continuous compression technique. AJR Am J Roentgenol 2004;182:180–182.
21. Kim J, Zabih R. Automatic segmentation of contrast-enhanced time resolved image series. J X-Ray Sci Technol 2000;9:1–11.
22. Cline HE, Dumoulin CL, Lorensen WE, Souza SP, Adams WJ. Volume rendering and connectivity algorithms for MR angiography. Magn Reson Med 1991;18:384–394.